STUDY ON MECHANICAL PROPERTIES OF CONFINED CONCRETE BASED ON DIGITAL IMAGE CORRELATION TECHNOLOGY

XIAONIU YU , LINZHU SUN* , FANG YANG
[1]College of Architecture and Civil Engineering, Wenzhou University, Wenzhou, 325035, China

With a double-layer stirrup confined high-strength concrete column as study object, vertical loading experiments were conducted, and the strain field of the member during loading was measured dynamically using the digital image correlation technology. The experimental results show that, for double-layer stirrup confined high-strength concrete, the strain change differs greatly between the early and late stages of loading, being smooth in the early stage and active in the last stage. Through the analysis of the full-field strain of the member, the displacement grid diagrams and strain distribution contour plots at different stress levels were obtained. From the contour distribution was determined that, during loading, the strains in the member are different at different positions and they are also different at different time points at one position. There is a stress concentration area during loading, where a "strain rebound" phenomenon occurs after the stress reaches its peak. The strain calculation results also reveal that selecting different areas for calculation will have large influence on the calculation results regarding the overall strain of the member. In addition, the experiments also indicate that, due to its non-contact and full-field features, the digital image correlation technology is suitable for dynamic measurement of structural force, and it is a powerful means for deformation detection and health monitoring of a structure.

Keywords: *digital image correlation; double-layer stirrup; concrete; bearing capacity; strain rebound*

1. Introduction

Scholars from China and other countries have made many efforts for the application of digital image correlation based measurement technology in different fields. In 2001, Chevalier et al. [1] studied the mechanical behaviors in mono-axial and double-axial stretching of rub materials using the digital image correlation method, established a hyperelastic model to simulate the mechanical behaviors of rub materials, and obtained an approximate stress-strain relationship. In 2004, Yamaguchi et al. [2] employed the digital image correlation method to measure the surface roughness of objects, and Yang [3] used the digital speckle correlation in an experiment regarding anisotropic nuclear functional materials. In 2002, Ma et al. [4] analyzed the feasibility and superiority of using the white light digital image correlation method in observing the surface deformation of rock materials, and modified the general digital image correlation method according to the deformation features of the rock materials. Yao et al. [5] studied the mechanical behaviors of crack damage evolution and growth for a composite material with glass fiber and epoxy resin braided structure under three-point bending load using the digital image correlation method. In 2004, Fan et al. [6] used the digital image correlation method to study the stress and strain at crack tips of orthogonal anisotropic materials.

Researchers also thoroughly studied the application of the digital image correlation technology in concrete structures; Destrebecq et al. carried out cyclic loading onto a concrete beam, active in service for 25 years, through a four-point bending experiment using the digital image correlation (DIC) technology, which is an optical method that employs tracking and image registration techniques for accurate 2D and 3D measurements of changes in images, and analyzed the influence of cracks and external environment on the useful life of the beam [7]. Shih and Sung studied reinforced concrete beams through three-point bending experiment, to demonstrate the feasibility of applying DIC technology in assessing reinforced concrete members, and highlighted that if finite element is used to deal with the cracks at stress concentration points, then the DIC equipment can accurately determine the positions of the cracks and can identify non-observable cracks and predict the development trend of the cracks [8]. The DIC equipment can precisely detect the crack development process at any time, while

* Autor corespondent/*Corresponding author*,
E-mail: xnyu09@163.com, xnyu@wzu.edu.cn

the acoustic emission (AE) equipment can locate the sources of cracks, and the combination of both DIC and AE equipment increase the quality of the results. Aggelis et al. studied the damage mechanism of concrete beams using both DIC and AE technologies, for example, the surface strain field, transient changes and elastic waves of the specimens need to be determined [9]. Rouchier et al. quantified the full-field displacement mappings, damage and fractures of carbon fiber reinforced concrete also using both AE and DIC [10]. Verbruggen et al. studied the four-point bending properties of carbon fiber and geotextile reinforced concrete beams, and the experiments showed that DIC can describe the surface crack development status, therefore having an important role in non-destructive detection [11].

With this method, this paper studies the force process in double-layer stirrup confined concrete and analyzes the strain change at different stresses.

2 Experimental processes and methods

(1)The equipment used in the experiments was a WAW-10000F electrohydraulic servo multi-function experimental loading system which recorded the real-time stress during the experiments, DIC equipment (used to determine strain), and a 12*9*50 mm calibration board which was used to conduct calibration before the experiments. The experimental loading system and the DIC equipment were used synchronously to ensure the correspondence relationship in time of the information acquisition. The experiments employed displacement control, the loading rate was 0.3 mm/min, and the acquisition rate of the DIC equipment was 10 frames/second. (2)According to the specifications of ASTM C39, we laid out the specimens by category first, and then leveled the ends of the 150 mm × 300 mm cylindrical specimens. The load on each specimen is measured using a NYL5000B servo-loading tester. Digital image correlation (DIC) was performed during tensile loading tests of fibre reinforced mortar samples. The full-field displacement mappings obtained by DIC revealed all ranges of cracks, from microscopic to macroscopic.

The experimental material was a concrete square column, measuring 250*250*1200 mm, with two layers of stirrup for confining, both inner and outer layers being square. Diagram of the test device, as shown Fig. 1. The characteristics of the material, including stirrup spacing, were presented in Table 1. The surface of the cast member was brushed with white coating and sprayed with black speckles. The speckle diameter is important considering that a large of the speckle can cause reduction in strain measurement accuracy, while a small diameter of the speckle would not allow an adequate differentiation in data acquisition by the DIC device. The member was fabricated with C60 high-strength concrete, which was stirred forcibly using a stirring machine. And it was compacted evenly up and down using a vibrating spear in loading into the die to ensure the evenness of the whole member, which was cast using an iron die, and it was artificially cured for 7 d and cured for 28 d through watering in natural conditions after shaped.

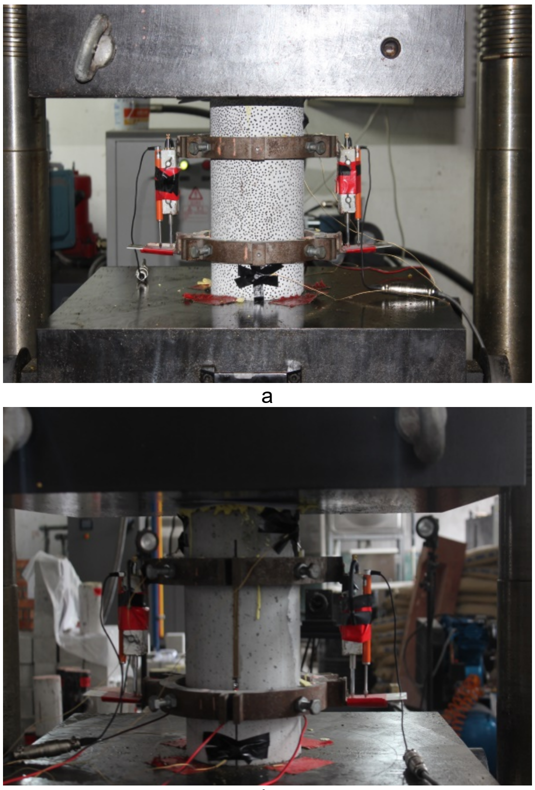

a

b

Fig. 1 - Diagram of the test device: (a)front, (b)rear.

Table 1

Table of specimen reinforcement.

Parameter	Characteristic	Parameter	Characteristic
Specimen dimensions /mm	250*250*1200	Outer stirrup diameter /mm	Φ8
Concrete strength class	C60	Spacing /mm	35
Longitudinal reinforcement strength class MPa	HRB335	Inner stirrup diameter /mm	Φ8
Stirrup strength class MPa	1200	Spacing /mm	50
Outer layer longitudinal reinforcement	8Φ12	Inner diameter of outer layer of stirrup /mm	230
Inner layer longitudinal reinforcement	8Φ10	Outer diameter of inner layer of stirrup /mm	150
Thickness of outer reinforcement protection layer	20mm		

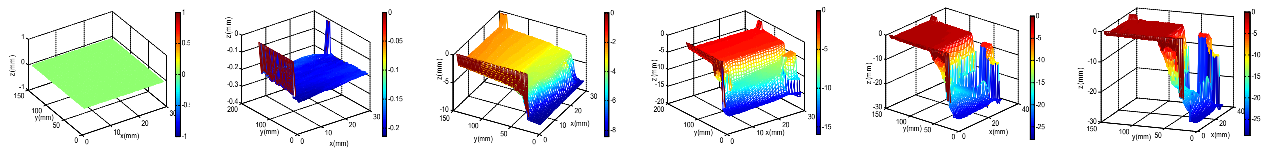

(a) Initial state (b) 20% stress level (c) 40% stress level (d) 60% stress level (e) 80% stress level (f) 100% stress level

Fig. 2 - Vertical displacement (axis y) at different stress levels.

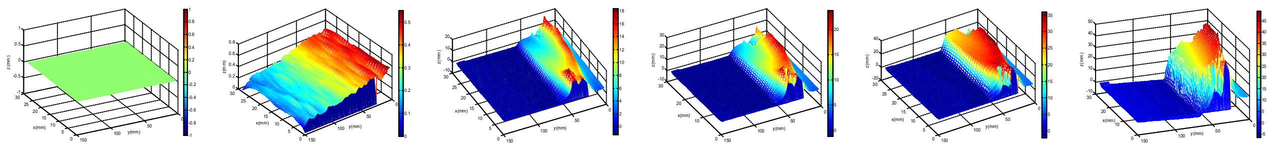

(a) Initial state (b) 20% stress level (c) 40% stress level (d) 60% stress level (e) 80% stress level (f) 100% stress level

Fig. 3 - Out-plane displacement (axis z) at different stress levels.

3. Analysis of experimental results

3.1 Analysis of displacement field on member surface

Figure 2a–f shows the displacement evolution status at different stress levels by the DIC user analysis software. From Fig. 2a, it can be seen that, in the initial state, all full-field displacements from the whole observation plane are 0 (light green). When the stress is loaded to 20%, the full-field displacements are still relatively even, roughly distributed between [-0.15– -0.2 mm]. Load deformation of materials is produced under low stress, however, the stirrup does not yield [11]. The protruding part with dark color at x=0 on the margin of the figure is caused by the margin effect of the analysis area, and is not considered in post-processing.

From the displacement grids in Figs. 2c–d (40% and 60% stress level), it can be seen that the displacements in the upper part of the member differ greatly from those in the lower part, and the displacement does not increase evenly from the upper part to the lower part, indicating that the member itself is not under even force. When the behavior of the displacement at 80% and 100% stress level, a common phenomenon that the displacement in a small area in the upper part of the member changes from large to small, to generate rebound, as shown in Figures 2d–f. This behavior can be explained considering that the member has complete structure and high bearing capability, and although the stress is relatively high and the strain increases constantly at the early stage, the stirrup starts to yield and the protection layer warps up to come off resulting in structural damage, the stress at the coming-off position is re-distributed and starts to dissipate and the strain generates rebound.

Figure 3 shows the grid diagrams of z plane displacement at different stress levels. The initial state of loading onto the member (Fig. 3a), and it can be seen from the colorimetric card that the full-field strain is 0. It can be seen from the evolution process in Figs. 3b–f that the peak strain in the member increases constantly from 0.5 mm at 20% stress level to 40 mm at 100% stress level because the full-field displacement mappings obtained by DIC revealed all ranges of cracks, from microscopic to macroscopic [11]; the strain increase amplitude varies with area and the displacement in the Z direction in the top of the member is far larger than that in the bottom of the member. The upper protection layer of the member starts to come off, because of structural damage occurs under too high stress.

3.2 Analysis of vertical strain at different stress levels

Through analysis of the vertical strain e_{yy} at different stress levels, the strain contour plots were obtained (Fig. 4). As can be seen from the figure, at different stress levels, the strain in the member has an overall trend of increasing; however, in a specific area, the strain does not increase all the time with the increase in stress. During the increase in stress, the dislocation (In materials science, dislocation is a crystallographic defect or irregularity within a crystal structure.), and crack development (The material under the cracks of the materials can continue to produce under load action.), etc. in the concrete crystal of the member cause re-distribution of stress and the strain change varies constantly with the re-distribution of stress. The full-field contour plots are divided into

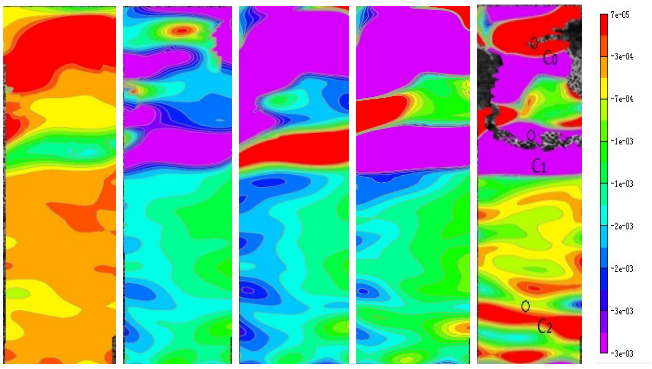

a.20% b.40% c.60% d.80% e.100%

Fig. 4 - The full-field strain contour plots at different stress levels.

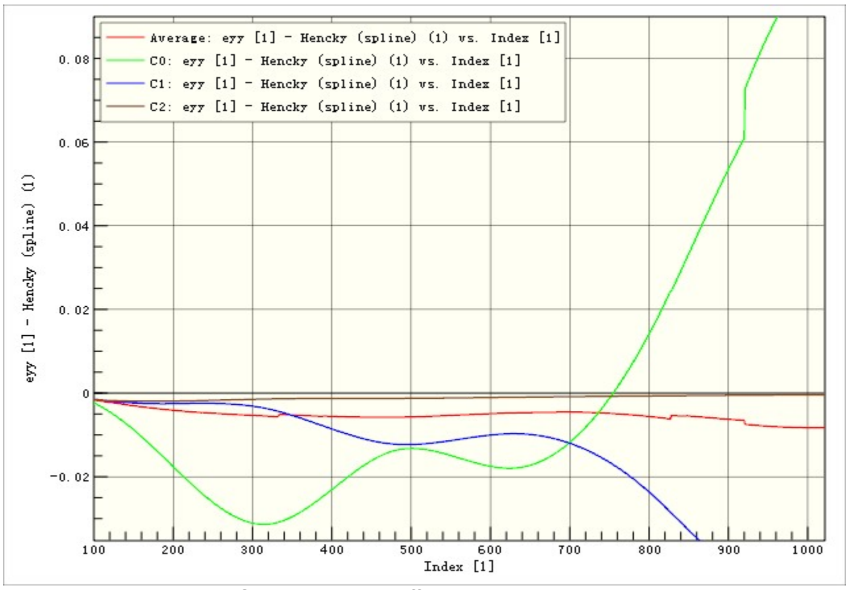

Fig. 5 - Strain curves at different locations.

different areas by contour lines. Different areas have different colors but two adjacent areas have continuous color transition process, and contour lines varies constantly that distribution does not have a law. The reason is the distribution of various materials is different in the concrete crystal of the member. In summary, the strain in two adjacent areas is continuous and the overall strain distribution in the member varies with the distribution of stress.

Only from Fig. 4e, it can be seen that the upper protection layer of the member starts to come off under too high stress, and the area with protection layer coming off generates a “strain rebound” phenomenon due to re-distribution of stress; such strain rebound is reflected by the reversion of color in the contour plot of this area, and the displacement rebound in Figs. 2 and 3 also works in concordance with this phenomenon. It can also be seen from Fig. 4 that, through the continuity of contour plot change, the development trend of structural damage can be predicted and the whole process of member damage evolution can be described during the analysis. This process indicates that the strain change at the late stage is evidently more active than at the early stage for double-layer stirrup confined high-strength concrete under pressure, which just conforms to the pressure characteristic of high-strength concrete.

4. Discussion about strain relaxation phenomenon

Figure 5 shows the curves of vertical strain obtained through spline interpolation fitting at three different positions, i.e., upper, middle and lower, of the member, where C_0, C_1, C_2, and $\mathrm{Average}$ represent the strains at upper, middle and lower sampling points, and their average strain, respectively. It is obvious that, at the early stage, the strain at the upper point C_0 increases rapidly due to stress concentration and is far higher than that at other two points, but at the late stage, the protection layer comes off, and the strain turns from negative to positive, with a “strain rebound” phenomenon occurring. Moreover, the calculation results also indicate that if there is a “strain rebound" phenomenon occurring in the data area selected for calculation, the strain rebound will lead to an error in measuring the overall strain of the member, so the selection of an area is very important in selecting output of strain, and it shall be conducted according to the actual situation. If the average strain at three points, i.e., the Average curve, is taken in the sense of statistical average, then the taken strain value is too small, and the conclusion will have bias towards unsafety at a weak location of the structure; however, if the maximum strain in the whole area is taken to represent the overall strain of the member, the conclusion is too conservative. The strain calculation area shall be selected according to the actual situation for analysis of the overall strain of the member; otherwise, the conclusion may have deviation.

5. Conclusions

In this paper, through numerical analysis of vertical bearing experiments of a double-layer stirrup confined high-strength concrete column. Double-layer stirrup confined high-strength concrete, the strain change differs greatly between the early and late stages of loading, being smooth in the early stage and active in the last stage. The strains in the member are different at different positions and they are also different at different time points at one position during loading. Selecting different areas for calculation will have large influence on the calculation results regarding the overall strain of the member. The digital image correlation technology is suitable for measurement with high requirements for full-field and real time, it can accurately analyze the three-dimensional displacement of any point within the range caught by the equipment lens, and it provides a nondestructive monitoring means for health monitoring and damage evolution of structures.

Acknowledgements

This work was supported by the National Key Research and Development Plan of China (No. 2016YFC0800209), the National Nature Science Foundation of China (No. 51508415, 51378398, No.51178356), Natural Science Foundation of Zhejiang Province (LQ15E080006), and the Plan Project of Science and Technology of Wenzhou (No. S20150010).

REFERENCES

1. L. Chevalier, S. Calloch, F. Hild, Digital image correlation used to analyze the multiracial behavior of rubber-like materials, European Journal of Mechanics A / Solids, 2001, **20**(2), 169.
2. I. Yamaguchi, K. Kobayashi, L. Yaroslavsky, Measurement of surface roughness by speckle correlation, Optical Engineering, 2004, **43**(11), 2753.
3. Yang, N. DSCM experiment and analytical study for the fracture behavior of anisotropic nuclear graphite [D]. Tianjin, Tianjin University, 2002 (in Chinese)
4. S.P. Ma, G.C. Jin, Y.S. Pan, Study on the white light DSCM method for deformation measurement of rock materials, Journal of Experimental Mechanics, 2002, **17**(1): 10 (in Chinese).
5. X.F. Yao, B.S. Lin, Z.Y. Zhang, Crack damage and growth behavior of braided composite, Engineering Mechanics, 2002, 19(5), 118 (in Chinese).
6. X.S. Fan, PhD thesis, The research of digital speckle correlation method, China, 2004.
7. J.F. Destrebecq, E. Toussaint, E. Ferrier, Analysis of cracks and deformations in a full scale reinforced concrete beam using a digital image correlation technique, Experimental Mechanics, 2011, **51**, 879.
8. M.H. Shih, W.P. Sung, Application of digital image correlation method for analyzing crack variation of reinforced concrete beams, Sadhana, 2013, **38**(4), 723.
9. D.G. Aggelis, S. Verbruggen, E. Tsangouri, T. Tysmans, D. Van Hemelrijck, Characterization of mechanical performance of concrete beams with external reinforcement by acoustic emission and digital image correlation, Construction and Building Materials, 2013, **47**, 1037.
10. S. Rouchier, G. Foray, N. Godin, M. Woloszyn, J.J. Roux, Damage monitoring in fiber reinforced mortar by combined digital image correlation and acoustic emission, Construction and Building Materials, 2013, **38**, 371.
11. S. Verbruggen, D.G. Aggelis, T. Tysmans, J. Wastiels, Bending of beams externally reinforced with TRC and CFRP monitored by DIC and AE, Composite Structures, 2014, **112**(1), 113.

****